

1-DEOXYNOJIRIMYCIN, A GLYCOSYLATION INHIBITOR INFLUENCES THE EXPRESSION OF EXTRACELLULAR MATRIX PROTEINS IN OSTEOSARCOMA CELLS

ZULAIKA ROSLAN¹, MUDIANA MUHAMAD², LAKSHMI SELVARATNAM³ & SHARANIZA AB-RAHIM^{4*}

^{1,2,4}Department of Biochemistry and Molecular Medicine, Faculty of Medicine, Universiti Teknologi MARA, Selangor Branch, Sungai Buloh Campus, 47000 Sungai Buloh, Selangor, Malaysia,

¹Institute of Medical and Molecular Biology (IMMB), Faculty of Medicine, Universiti Teknologi MARA, Selangor Branch, Sungai Buloh Campus, 47000 Sungai Buloh, Selangor, Malaysia,

³Department of Biomedical Sciences (Anatomy), School of Medicine and Health Sciences, Monash University Malaysia, Jalan Lagoon Selatan, 47500 Bandar Sunway, Selangor, Malaysia.

sharaniza_abraham@uitm.edu.my

ABSTRACT

Malignant tumour cells secrete extracellular matrix (ECM) proteins with growth factors and cytokines to promote cell motility and adhesion for metastasis. The cell-ECM adhesion sites are comprised of integrin-bound ECM proteins, which are glycoconjugates, susceptible to the aberrant glycosylation resulting in alterations of cell-ECM adhesion dynamics. Inhibition of glycosylation could decrease the rate of invasiveness in metastatic tumour cells like osteosarcoma (OS), of which the underlying mechanism is still unknown. Hence, this study aims to determine the effect of glucosidase inhibitors towards the expression of ECM proteins in metastatic OS cell lines. OS cells (MG63) were treated with 0.5 mM of 1-deoxynojirimycin (1-DNJ). Analyses such as the glycosylation assay, ECM-cell adhesion assay, scratch assay, and Western blot analysis were performed after a 24-h treatment for each respective sample. The expression level of glycosylated proteins was the highest in non-treated MG63 cells. The cell migration rate was increased in MG63 cells treated with 1-DNJ compared to the normal osteoblast cells. The cell adhesion assay results showed an increased rate of cell adhesion towards vitronectin but decreased adhesion rate towards collagen (types I, II, and IV), fibronectin, laminin, and tenascin in 1-DNJ-treated OS cells. Western blot analysis presented a high expression level of fibronectin, vitronectin, and collagen type II in both non-treated and treated groups of MG63 cells. The inhibitory effect of 1-DNJ upregulates ECM remodelling by disrupting integrin from binding to the ECM proteins, subsequently increasing the migration rate of metastatic OS cells.

Keywords: Extracellular matrix protein, 1-Deoxynojirimycin, integrin glycosylation, cell adhesion rate, migration assay.

Introduction

Approximately 1000 cases of osteosarcoma (OS) are reported annually in the United States, which predominantly affect children and adolescents between 10 and 20, although a bimodal age distribution could be seen after 65 years of age following a second peak of invasion (American Cancer Society, AICR, 2020). Despite advances in multimodal therapy, OS disease management remains challenging due to its high rate of metastasis, whereby 30% to 40% of patients experienced relapse (Ben Kridis et al., 2022) and 20% presented with metastasis upon first diagnosis (Zhang et al., 2019). The rapid disease progression of OS imposes poor prognosis, as indicated in the reduced survival rate by 20% following lung metastasis (Rathore & Van Tine, 2021). Nonetheless, the mechanism attributable to metastatic OS remains incomprehensive due to involvement of multiple cellular proteins tightly regulated by their own signalling pathway.

The invasion by malignant cells is initiated by a signalling pathway that regulates interactions between the cytoskeletal network and cell-extracellular matrix (ECM) concurrently with cell-cell interactions, resulting in various cell-ECM adhesion strength (Masi et al., 2020). Reorganisation of malignant cell attachment to the ECM enables their dissociation from the original tumour mass, leading to the degradation of surrounding ECM and tissue invasion or intravasation into blood vessels, travelling to distant cells through the circulation (Welch & Hurst, 2019). The binding of cells to the ECM is mainly provided by the transmembrane integrin receptor, which involves interaction with ECM ligands (ECM proteins) including fibronectin, laminin, and collagen (Doyle et al., 2022). Similarly, vitronectin, another type of adhesive glycoprotein, has been reported as a link between cells and ECM through integrins (Burgos-Panadero et al., 2019).

The involvement of integrin in metastasis is highly relevant, as reported recently, whereby inhibition of alpha-5 beta-3 integrin impaired cell adhesion and hindered cell migration in MDA-MB-231 malignant breast cancer cell lines (Altei et al., 2020). More importantly, integrins and the ECM proteins are glycoconjugates, mostly comprising of N-glycans, O-glycans, and glycosaminoglycans that represent extreme structural diversity, contributing to the dynamic interactions between integrin and the ECM network (Marsico et al., 2018). Although glycosylation is tightly regulated due to the vast diversity and complex characteristics of glycans on the resulting glycoconjugates, any dysregulation of the process could lead to the impairment of a glycoprotein crucial for normal cellular function, leading to pathological condition if neither detected nor corrected (Reily et al., 2019). Nonetheless, many compounds exert an inhibitory effect towards glycosylation, one of which is the 1-deoxynojirimycin (1-DNJ), an iminosugar also known as duvoglustat or moranoline, reported as a potent α -glucosidase inhibitor (Wang et al., 2020). For instance, the inhibition of metastatic B16F10 melanoma cells is indicated by a significant decrease in cell adhesion and migration rate, reducing invasion and cell-matrix adhesion through the suppression of MMP2 and MMP9 activities and expression (Wang et al., 2010).

While aberrant glycosylation is indisputable for cancer progression, the dysregulation of ECM remodelling is inevitable for malignant cell migration and invasion. The imperative associations between these events during metastasis have been well documented in other cancers but remain elusive for OS. Therefore, this study aims to investigate the effect of aberrant glycosylation inhibition on the malignancy capacity of OS cells. It is hypothesised that inhibition with α -glucosidase inhibitor (1-DNJ) influences the organisation of the cell-ECM adhesion, hence modulating the aggressiveness of cancer cells. The outcome of this study will contribute

to a better understanding of the underlying mechanism for OS metastasis towards the development of potential OS therapeutics.

Materials and Methods

Cell culture

Human OS cells, MG63, were purchased from the American Type Culture Collection (ATCC, USA) and sub-cultivated regularly in 1× Dulbecco's modified Eagle medium F12 (DMEM-F12) growth medium with phenol red, supplemented with 10% foetal bovine serum (FBS), 100 mg/mL of penicillin G, and 100 mg/mL of streptomycin (Nacalai Tesque, Japan) at 37°C in a humidified incubator at 5% CO₂. Normal human osteoblast cells, hFOB1.19 (ATCC, USA), were maintained in DMEM-F12 without phenol red (Nacalai Tesque, Japan) supplemented with a similar composition to the MG63 cells and incubated in the CO₂ incubator.

The inhibitor

The α-glucosidase-I/II inhibitor, 1-DNJ, was purchased from Cayman Chemical (Cayman Chemical, USA). The concentrated stock was prepared using a purged DMSO to avoid oxidation. The DMSO (Sigma Aldrich, USA) was placed in a tightly closed hypoxia incubator chamber (Billup-Rothenberg, USA), with the gas inlet connected to the nitrogen gas supply. The gas pressure was set at two psi. The oxygen gas inside the chamber was released through the gas outlet by allowing the nitrogen gas to flow inside the chamber through the gas inlet for 3 min, by which both the gas inlet and outlet were clamped simultaneously to stop the gas flow. Subsequently, the DMSO was incubated inside the chamber for 10 min per 1 mL of solvent. After incubation, the gas inlet was opened, followed by the gas outlet to de-gas the chamber. The purged DMSO was then used to dissolve the 1-DNJ into 50 mM stock concentration and stored at -20°C until further use.

Glycosylation assay

Glycosylated proteins in the control sample (hFOB1.19 cells) and test sample (MG63 cells) were detected using the Glycoprotein Staining Kit (PIERCE, Thermo Scientific, USA). Prior to the assay, both cells were treated with 0.5 mM of 1-DNJ for 24 h at 37°C in a humidified incubator at 5% CO₂, according to Mustafa and colleagues, hence why only one concentration was used (Mustafa et al., 2019). The non-treated cells were also incubated in the same condition. Subsequently, the total cellular protein was extracted using the RIPA lysis buffer. The cells were washed twice with ice-cold 1× PBS (Sigma-Aldrich, USA) and enzymatically detached using trypsin (Nacalai Tesque, Japan), followed by centrifugation at 252 × g for 5 min at 20°C. Cell pellets were resuspended with 500 µL of 1× ice-cold RIPA buffer (PIERCE, USA) premixed with protease inhibitor (Thermo Scientific, USA), followed by constant agitation on the orbital shaker at 4°C for 30 min. Next, the cell suspension was sonicated in a water-bath sonicator for 20 min on ice and centrifuged at 10000 × g for 20 min at 4°C. Finally, the supernatant containing the protein was aspirated into new tubes, and quantification was performed using the Bradford protein assay kit (Bio-Rad, USA).

For the glycosylation assay, 100 µg of isolated protein from each group of cells (treated and non-treated) was separated via SDS-PAGE (80 V; 1 h and 30 min) in the presence of bovine serum albumin (BSA, positive control) and soya bean (negative control). Subsequently, the gel was fixed by complete immersion in 100 mL of 50% methanol for 30 min. The methanol solution was then discarded and replaced with 100 mL of 3% acetic acid for 10 min before being washed twice with ultrapure water by gentle agitation for 10 min. The gel was transferred to a tray containing 25 mL of oxidising solution and gently shaken for 15 min, followed by three

times washing with 100 mL of 3% acetic acid by gentle shaking for 5 min. The gel was then transferred into 25 mL of reducing solution for 5 min before the final step of extensive washing with 3% acetic acid, followed by ultrapure water. The glycoproteins were then visualised using the Gel Doc (Bio-Rad, USA) imaging system.

Scratch assay

The scratch assay was performed post-24-h treatment with 1-DNJ at the concentration of 0.5 mM. Monolayers of the MG63 and hFOB1.19 (control) cells at 3.0×10^5 cells per well in the 6-well culture plate were treated with 1-DNJ (0.5 mM) in the CO₂ incubator. At the end of the 24-hour incubation, the treatment media was discarded. The monolayer was scratched by drawing a straight line at a 45° angle in the middle of the well with a 200- μ L yellow micropipette tip. The scratching was also performed on the non-treated cells post-24-h culture, assigned as the negative control. Subsequently, 5 mL of maintenance medium was added to each well before further incubation at 37°C in a CO₂ incubator. The morphology of the cells was observed and recorded for any differences at 0 h (immediately after scratching) and at 24- and 48-h post-scratch. Estimation of the value corresponding to the scratched area was measured using the Image J software (NIH, USA).

Extracellular Matrix (ECM) adhesion assay

The rate of cell adherence to the ECM was measured using the ECM Cell Adhesion Array Kit (Chemicon International, Canada) according to the protocol by the manufacturer. The MG63 cells in a 96-well plate (1.0×10^5 cells/well) were washed thrice with 200 μ L of the assay buffer. Next, 100 μ L of the cell stain solution was added to each well, followed by a 5 min incubation at room temperature. Then, the cell stain solution was discarded, and the plate was gently washed with deionised water five times before being air-dried for several minutes. Subsequently, the extraction buffer was added to each well, and the plate was incubated on the orbital shaker at room temperature for 10 min until the cell-bound stain was completely solubilised. Finally, the absorbance was measured at the wavelength between 540–570 nm on the microplate reader Victor 5 (PerkinElmer, USA).

Western blot analysis

The expression of target proteins was determined by Western blot analysis. Total cellular protein was isolated from the non-treated (control) and treated with 1-DNJ cells. Treatment of the compound was performed at the concentration of 0.5 mM for 24 h at 37°C in a CO₂ incubator. After a 24-hour incubation, the treatment media was removed, and the cells were washed twice with ice-cold 1 \times PBS, followed by enzyme trypsinisation. The detached cells were collected in a microtube and centrifuged at 10000 \times *g* for 5 min in a pre-chilled microcentrifuge. Subsequently, the supernatant was discarded, and RIPA buffer (PIERCE, Thermo Scientific, USA) was added to the cell pellet for cell lysis, followed by the addition of Protease Inhibitor Mini Tablet (PIERCE, Thermo Scientific, USA). The concentration of isolated proteins was quantified using the Bradford protein assay kit (Bio-Rad, USA). Approximately 200 μ g of total cellular protein was loaded into each well and subjected to SDS-PAGE of 12% gel at 80 V with a running time of 1 h and 30 min. The separated proteins were transferred onto a 0.2 μ m nitrocellulose membrane for immunoblotting, followed by blocking with 5% BSA diluted with 1 \times TBST for 1 h at 4°C and subsequently an overnight incubation at 4°C with monoclonal primary antibodies for fibronectin, vitronectin, collagen type II, and beta-actin (1:1000 ratio; Abcam, USA). After the incubation, the membrane was washed with 1 \times TBST thrice before being incubated at 4°C with the secondary conjugated-HRP antibody (1:1000 ratio) for 1 h. Finally, the conjugated membrane was immersed in SuperSignal™ West Pico PLUS Chemiluminescent Substrate (Thermo Scientific, USA) for 5 min for protein band

visualisation and captured using an immunoscanner (Li-COR, USA), followed by quantification using MyImage Analysis software (Thermo Scientific, USA).

Statistical analysis

Each assay was repeated three times independently, and the data were presented as mean \pm standard deviation (SD). Statistical analysis was performed by one-way ANOVA test and further compared with Tukey's comparison multiple tests by GraphPad Prism Software (Version 9.0.0, San Diego, California, USA), and the value of $p < 0.05$ was regarded as significant.

Results and Discussion

Presence of glycosylated proteins via glycosylation assay

Glycosylated protein detection was expressed as a single band in the SDS-PAGE gel profile, as shown in Figure 1. Although the intensity of the bands detected for all samples is not relatively comparable to that of the positive control (BSA), the level of expression is the highest in MG63 cells when compared with the normal osteoblasts hFOB1.19, followed by the band separated from MG63 cells treated with 1-DNJ. No remarkable difference is observed in the intensity between the 1-DNJ treated with the control cells (HFOB1.19), whereby both bands appeared as less intense than the MG63 cells.

Despite the importance of glycosylation towards rendering functional proteins, aberrant glycosylation is attributable to an elevated rate of cancer cell invasion, eventually leading to rapid metastasis (Oliveira-Ferrer et al., 2017). Unlike normal cells, cancer cells comprise several alterations in their glycoconjugate counterparts with specific modifications, stimulating tumour cell invasiveness and, consequently, metastasis to secondary sites (Pinho & Reis, 2015). Such process has been documented for breast and colon cancers, but knowledge on the role of aberrant glycosylation in solid tumour cancer like OS is still lacking. Moreover, aberrant glycosylation imposes on the interactions between integrin and the ECM network. Therefore, this study investigated the association between aberrant glycosylation and integrin by disrupting glycosylation with an α -glucosidase-I/II inhibitor, 1-DNJ. Despite the absence of prior reports on glycosylated proteins in OS cells, their presence was evident not only in the MG63 cells but also in the normal osteoblast cells (hFOB1.19), as indicated by the glycosylation assay result in Figure 1. More importantly, the intensity of the band was reduced prominently in cells treated with 1-DNJ than the non-treated MG63 cells, indicating the inhibitory activity of the compound. Until recently, no one has ever used the α -glucosidase-I/II inhibitor 1-DNJ as a glycosylation inhibitor in OS, particularly in MG63 cells.

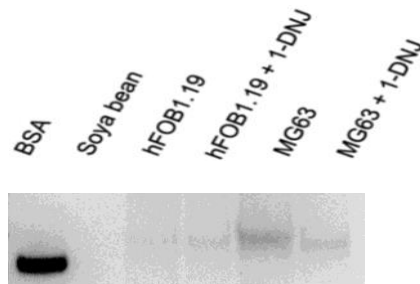


Figure 1: The SDS-PAGE gel profile of glycosylation assay. A single band is detected in all samples, indicating the presence of glycosylated proteins. Lane 1: Positive control (BSA); Lane 2: Negative control (soya bean); Lane 3: hFOB1.19 cells; Lane 4: hFOB1.19 cells treated with 1-DNJ at 0.5 mM; Lane 5: MG63 cells; Lane 6: MG63 cells treated with 1-DNJ at 0.5 mM.

Rate of cell migration via scratch assay

The area of closure at post-scratch time (h) was referred to as the remaining area uncovered by the cells, expressed as fold value over time. Compared with the control hFOB1.19 cells, treatment with 1-DNJ increased the rate of migration, presented by the total wound closure at 24-h post-treatment (Figure 2) and a significant decrease in the fold value of 0.03 ($p < 0.05$) against 0.18 ($p < 0.05$) for the non-treated hFOB1.19 cells (Figure 3a). The rate of migration of the MG63 cells is significantly decreased compared to the control, indicated by the large, uncovered area (Figure 2), with a higher fold value of 0.76 ($p < 0.05$), as shown in Figure 3b. A similar pattern of reduced migration rate is observed in MG63 cells treated with 1-DNJ, with a significant fold value of 0.63 ($p < 0.05$, Figure 3b), higher than that of the control. However, the rate of migration is significantly increased when the 1-DNJ-treated MG63 cells are compared against the non-treated MG63 cells, shown as almost total closure at 48-h post-treatment (Figure 2) and presented by the decreased fold value from 0.71 to 0.46 ($p < 0.05$, Figure 3b).

Glycosylated proteins are detected not only in the OS (MG63) cells but also in the normal osteoblast cells (hFOB1.19), as depicted in the glycosylation assay result in Figure 1. More importantly, the intensity of the band was reduced prominently in cells treated with 1-DNJ compared to the non-treated MG63 cells, indicating the inhibitory activity of the compound. Subsequently, the scratch assay (wound assay) was performed to assess the 1-DNJ inhibitory effect on the rate of migration of the normal osteoblast hFOB1.19 cells and metastatic MG63 cells against the control.

The result of the scratch assay showed that, compared to the control, inhibition of the hFOB1.19 cells with 1-DNJ significantly increased the cell migration rate, indicated by the total wound closure after 24 h of compound treatment. The rapid migration rate of the normal osteoblast cells corroborated with the wound healing mechanism, involving collective migration of cells in a two-dimensional confluent monolayer, whereby cells adjacent to the wound margin became highly polarised due to the force by the actin cytoskeleton. Subsequently, the cells progressed into pseudopodium-like outward projections into the free space before detachment for migration (Whitelaw et al., 2020). Compared with the control, the reduced migration rate of the non-treated MG63 cells was anticipated since tumour cells require a longer transition time from the sessile to the polarised state, resulting in a slower onset of migration (Sigismund et al., 2021). Nevertheless, the rate of cell migration in the MG63 cells treated with 1-DNJ was unexpectedly higher than the control. This could be attributed to the inhibition of alpha-glucosidase-I/II of the integrin, which disrupted binding towards the ligands or ECM proteins and increased the dissociation between the ECM and cytoskeleton (Park et al., 2020), consequently increasing the rate of migration.

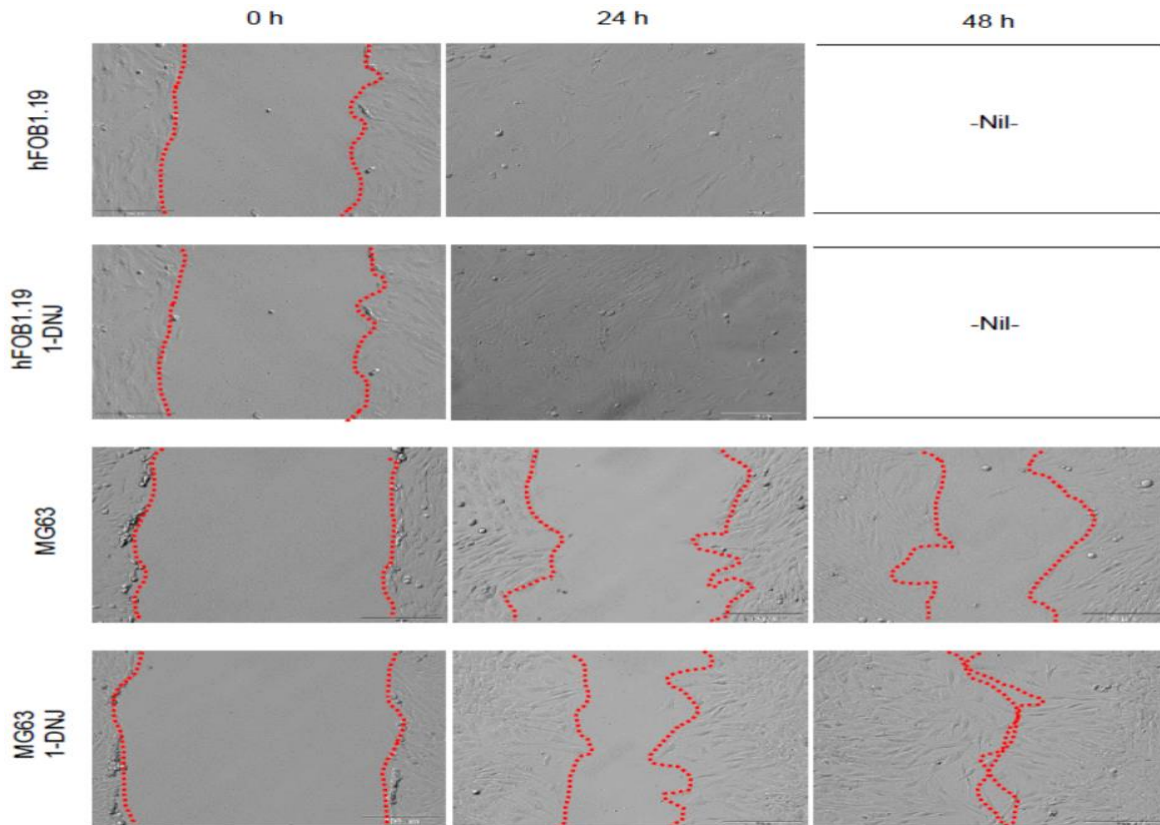
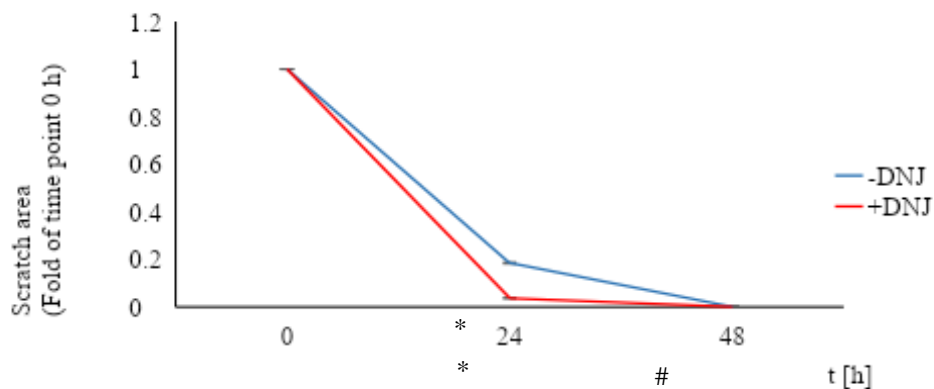


Figure 2: Presentation of scratched areas in the test samples. The width of the scratched area is calculated as the average distance between the edges of the scratch, which decreases over time, equivalent to the migration rate (values not shown). Inhibition with 1-DNJ in OS cells, MG63, increased the migration rate, indicated by the smaller area width left uncovered compared to that of the non-treated cells.

Rate of adherence of the ECM proteins via adhesion assay

The ECM Cell Adhesion Assay Kit (ECM540; Chemicon International, Canada) was utilised to assess the specific cell surface integrins towards the ECM proteins. The kit comprised of ECM proteins: collagen I (Col I), collagen II (Col II), collagen IV (Col IV), fibronectin (FN), laminin (LN), tenascin (TN), vitronectin (VN), and BSA as control. Except for VN, the result showed a higher percentage of cell adhesion towards all the other ECM proteins in the non-treated MG63 cells compared to the cells treated with 0.5 mM of 1-DNJ, as presented in Figure 4.



(a)

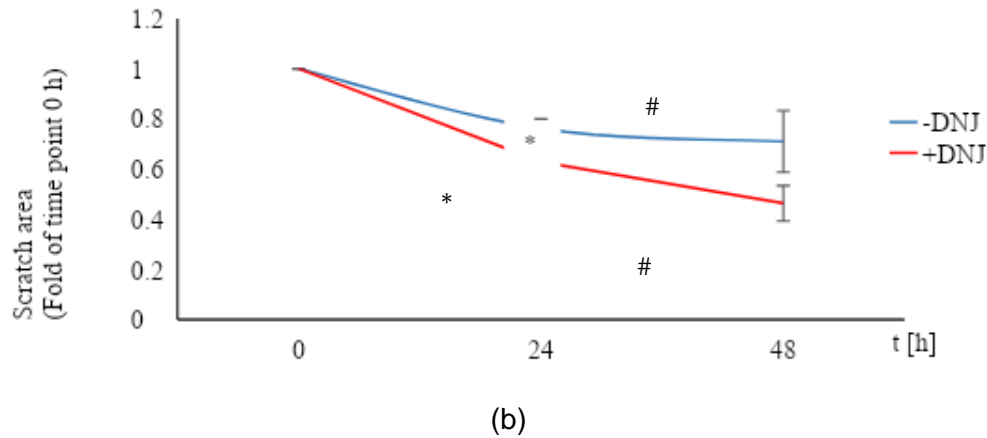


Figure 3: The closure of the scratched area. Closure of the scratched area is expressed as the remaining area uncovered by the cells in (a) hFOB1.19 and (b) MG63 cells. The scratched area at 0 h was set to 1. All data are presented as mean \pm SD, and each experiment was repeated three times ($n = 3$) per group. * $P < 0.05$ for 24 h vs 0 h; # $P < 0.05$ for 48 h vs 0 h.

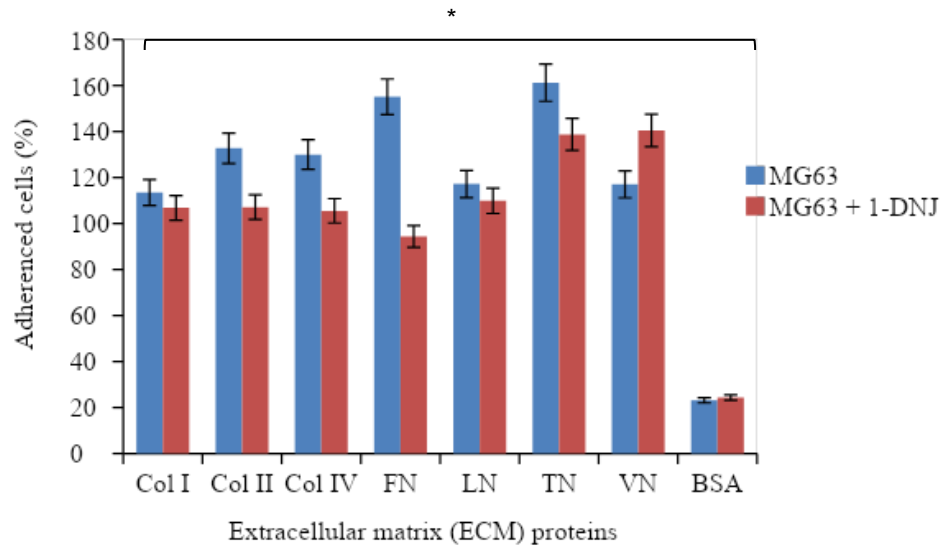


Figure 4: The percentage of cell adherence towards ECM proteins in OS cells. Adhered cells were compared between the non-treated MG63 cells and treated with 1-DNJ at 0.5 mM relative to BSA. All data are presented as mean \pm SD of three experimental replicates ($n = 3$). Non-treated cells showed a significantly higher percentage of adherence towards all ECM proteins, except for VN (* $P < 0.05$), compared to cells treated with 1-DNJ.

Except for vitronectin, the MG63 cell adhesion rate was elevated towards all the other ECM proteins. As reported with other malignancies, which had undergone various levels of ECM remodelling within the metastatic niche (Patras et al., 2023), the ECM remodelling was initiated by circulating tumour cells (CTCs) that secreted the integrins with abundant fibronectin and laminin towards endothelial cells deposition and assembly of fibrillar fibronectin (Kai et al., 2019). Meanwhile, being the major component of ECM, collagen and its subtypes indisputably dominate ECM remodelling (Diller & Tabor, 2022). In this study, OS cells exhibit the highest rate of adherence towards tenascin, which corroborated a previous report that the ECM protein was highly expressed in cancer tissues (Sun et al., 2018). The abundance of tenascin in metastasised cells is attributable to its multiple cellular sources, which include cancer cells,

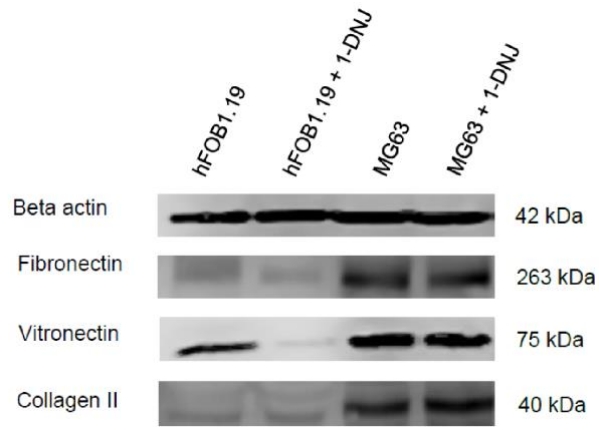
stromal cells, and vascular cells (Sun et al., 2019). Essentially, the CTC extravasation from the circulation into the new tissue for metastasis is dependent on the ECM remodelling, which involves the ECM proteins, thus increasing its secretion or expression within the metastatic cascade, concurrent with the finding in this study.

The dynamic interaction between integrin and the ECM was well described, particularly the post-translational modifications (PTMs), such as glycosylation of the ECM components glycosaminoglycan (GAG) and proteoglycan (PG). More importantly, integrins are also susceptible to glycosylation, with an increased chance of aberrancy during metastasis and eventually altering ECM remodelling (Singh et al., 2018). As a result, inhibition of the aberrant glycosylation by the 1-DNJ significantly reduced the percentage of adhered cells to ECM proteins, as demonstrated in this study. However, the result of vitronectin presented otherwise, whereby the percentage of adhered cells was increased significantly after inhibition with 1-DNJ instead of reduction, as with the other ECM proteins. A plausible explanation is the function of vitronectin, i.e., as the key controller of mammalian tissue repair and remodelling activity, following its detection in many tissues after exposure to trauma or stress (Goyal & Ta, 2020). Hence, this function could overcome the aberrant glycosylation and the inhibitory activity of 1-DNJ within the OS cells.

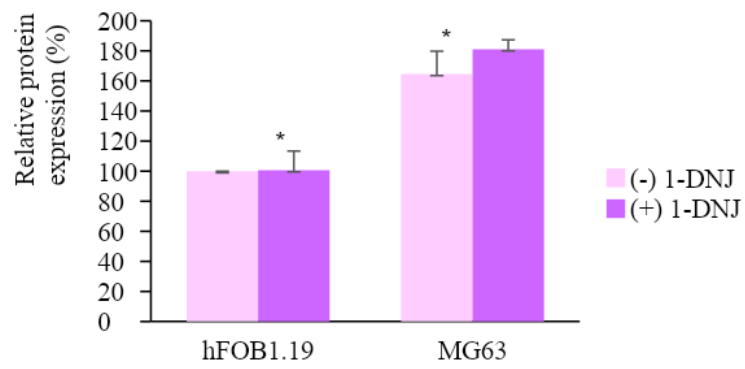
Expression of target proteins via Western blot analysis

Western blot analysis was performed for ECM proteins fibronectin, vitronectin, and collagen type II, and their level of expression in test samples was compared to that of the control, hFOB1.19 cells. The expression level of fibronectin at 263 kDa (Figure 5a) is higher in the non-treated and treated MG63 cells, with a significant difference of $p < 0.05$ against fibronectin expressed by the control (Figure 5b). No significant difference in the level of expression of vitronectin (75 kDa) is noted between both groups of MG63 cells with the control, as shown in Figure 5c. Meanwhile, Figure 5a shows the elevated expression level of collagen type II at 40 kDa in the non-treated and treated MG63 cells compared to the control, with a significant difference ($p < 0.05$) indicated by the histogram in Figure 5d. Although not significant, the hFOB1.19 cells treated with 1-DNJ presented lower expression levels for all three ECM proteins against the control (Figure 5a).

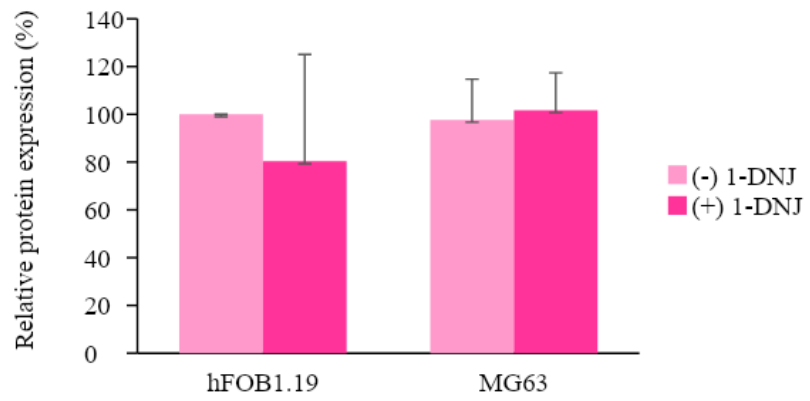
The level of expression of three ECM proteins in the metastatic OS cells (MG63) of both groups measured by Western blot was compared against the normal osteoblast cells (hFOB1.19). The result showed a significant increase in the expression of fibronectin and collagen type II in the non-treated group, which corroborated with the high percentage of cells that adhered to both ECM proteins. No significant change was seen for vitronectin expression in the same group, most likely the reason for the low percentage of cells abundant to this ECM protein, as measured by the ECM adhesion assay. Meanwhile, a contrasting level of expression for both fibronectin and collagen type II was seen in the MG63 cells treated with 1-DNJ. Although not significant, the elevated expression level could be attributable to the inhibitory effect of 1-DNJ, resulting in the upregulation of the ECM remodelling in the metastatic niche.



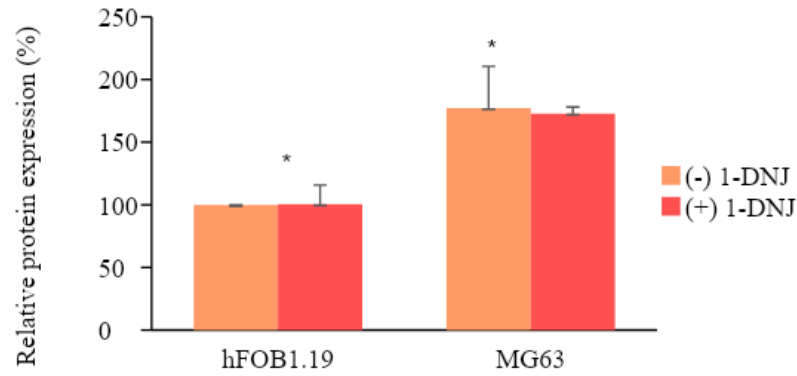
(a)



(b)



(c)



(d)

Figure 5: Western blot analysis of ECM protein expression in hFOB1.19 and MG63 cells of non-treated and 1-DNJ treated groups. (a) The ECM proteins fibronectin, vitronectin, and collagen type II are expressed at 263 kDa, 75 kDa, and 40 kDa. The level of expression of the ECM proteins (b) fibronectin, (c) vitronectin, and (d) collagen type II was compared with that of the control, hFOB1.19, by measuring the intensity of the bands. All data are presented as mean \pm SD of three experimental replicates (n = 3).

Conclusion

The aberrant post-translational modifications (PTMs) of the extracellular matrix (ECM) ligands in malignant cells that cause architectural modifications in the ECM rendered them a potential target for PTM inhibitors such as those used in this study. The findings of the study reveal that inhibition of alpha-glucosidase-I/II of the integrin disrupted the binding of the ECM proteins, resulting in the upregulation of ECM remodelling in metastatic OS cells. These current findings provide new insight towards the development of targeted therapeutic for OS through modulation of the integrin-ECM proteins association in tumour progression.

Findings

The effects of glycosylation on cell-matrix interaction by modifying the functions of anchoring proteins and extracellular basement membrane proteins including integrins, laminin, fibronectin, and collagen in the ECM are well established (Thomas et al., 2021). Thus, the observation on the effect of 1-DNJ on ECM is a preliminary result. To facilitate comprehensive future research, flow cytometry with scanning electron microscopy (SEM) techniques should be incorporated to further visualise the relationship between 1-DNJ effects and ECM proteins.

Contribution

In this study, the effects of 1-DNJ were observed on one concentration.

Acknowledgement

The authors would like to acknowledge the Institute of Medical Molecular and Biotechnology (IMMB) of Faculty of Medicine, Universiti Teknologi MARA (UiTM), Sg. Buloh Campus, Selangor.

References

- Altei, W. F., Pachane, B. C., Dos Santos, P. K., Ribeiro, L. N. M., Sung, B. H., Weaver, A. M., & Selistre-De-Araújo, H. S. (2020). Inhibition of $\alpha\text{v}\beta 3$ integrin impairs adhesion and uptake of tumor-derived small extracellular vesicles. *Cell Communication and Signaling*, *18*(1), 1–15. <https://doi.org/10.1186/s12964-020-00630-w>
- American Cancer Society |AICR. (2020). *About Osteosarcoma, What Is Osteosarcoma ?* <https://www.cancer.org/cancer/osteosarcoma.html>
- Ben Kridis, W., Ennouri, S., Khmiri, S., Keskes, H., Daoud, J., & Khanfir, A. (2022). Prognostic factors and treatment of relapsed osteosarcoma: A monocentric Tunisian retrospective study. *Archives de Pédiatrie*, *29*(4), 287–291. <https://doi.org/10.1016/j.arcped.2021.11.019>
- Burgos-Panadero, R., Noguera, I., Cañete, A., Navarro, S., & Noguera, R. (2019). Vitronectin as a molecular player of the tumor microenvironment in neuroblastoma. *BMC Cancer*, *19*(1), 1–10. <https://doi.org/10.1186/s12885-019-5693-2>
- Diller, R. B., & Tabor, A. J. (2022). The Role of the Extracellular Matrix (ECM) in Wound Healing: A Review. *Biomimetics*, *7*(3), 14–16. <https://doi.org/10.3390/biomimetics7030087>
- Doyle, A. D., Nazari, S. S., & Yamada, K. M. (2022). *Cell – extracellular matrix dynamics*.
- Goyal, U., & Ta, M. (2020). A novel role of vitronectin in promoting survival of mesenchymal stem cells under serum deprivation stress. *Stem Cell Research and Therapy*, *11*(1), 1–14. <https://doi.org/10.1186/s13287-020-01682-y>
- Kai, F., Drain, A. P., & Weaver, V. M. (2019). The extracellular matrix modulates the metastatic journey. *Physiology & Behavior*, *176*(1), 139–148. <https://doi.org/10.1016/j.devcel.2019.03.026>
- Marsico, G., Russo, L., Quondamatteo, F., & Pandit, A. (2018). Glycosylation and Integrin Regulation in Cancer. *Trends in Cancer*, *4*, 1–16. <https://doi.org/10.1016/j.trecan.2018.05.009>
- Masi, I., Caprara, V., Bagnato, A., & Rosanò, L. (2020). Tumor Cellular and Microenvironmental Cues Controlling Invadopodia Formation. *Frontiers in Cell and Developmental Biology*, *8*(October). <https://doi.org/10.3389/fcell.2020.584181>
- Mustafa, S. H., Muhamad, M., & Ab-Rahim, S. (2019). Aberrant N-glycosylation regulates invasion of MG-63 cells through extracellular matrix remodeling. *International Journal of Applied Pharmaceutics*, *11*(Special Issue 5), 75–79. <https://doi.org/10.22159/ijap.2019.v11s5.T0053>
- Oliveira-Ferrer, L., Legler, K., & Milde-Langosch, K. (2017). Role of protein glycosylation in cancer metastasis. *Seminars in Cancer Biology*, *44*, 141–152. <https://doi.org/10.1016/j.semcancer.2017.03.002>
- Park, E. J., Myint, P. K., Ito, A., Appiah, M. G., Darkwah, S., Kawamoto, E., & Shimaoka, M. (2020). Integrin-Ligand Interactions in Inflammation, Cancer, and Metabolic Disease: Insights Into the Multifaceted Roles of an Emerging Ligand Irisin. *Frontiers in Cell and Developmental Biology*, *8*(October), 1–17. <https://doi.org/10.3389/fcell.2020.588066>
- Patras, L., Paul, D., & Matei, I. R. (2023). Weaving the nest: extracellular matrix roles in pre-metastatic niche formation. *Frontiers in Oncology*, *13*(June), 1–20. <https://doi.org/10.3389/fonc.2023.1163786>
- Pinho, S. S., & Reis, C. A. (2015). Glycosylation in cancer: mechanisms and clinical implications. *Nature Publishing Group*, *16*(August), 540–555. <https://doi.org/10.1038/nrc3982>
- Rathore, R., & Van Tine, B. A. (2021). Pathogenesis and Current Treatment of Osteosarcoma: Perspectives for Future Therapies. *Journal of Clinical Medicine*, *10*(6), 1182. <https://doi.org/10.3390/jcm10061182>
- Reily, C., Stewart, T. J., Renfrow, M. B., & Novak, J. (2019). Glycosylation in health and disease. *Nature Reviews Nephrology*, *15*(6), 346–366. <https://doi.org/10.1038/s41581-019-0129-4>
- Sigismund, S., Lanzetti, L., Scita, G., & Di Fiore, P. P. (2021). Endocytosis in the context-dependent regulation of individual and collective cell properties. *Nature Reviews Molecular Cell Biology*, *22*(9), 625–643. <https://doi.org/10.1038/s41580-021-00375-5>
- Singh, C., Shyanti, R. K., Singh, V., Kale, R. K., Mishra, J. P. N., & Singh, R. P. (2018). Integrin expression and glycosylation patterns regulate cell-matrix adhesion and alter with breast cancer progression. *Biochemical and Biophysical Research Communications*, *499*(2), 374–380. <https://doi.org/10.1016/j.bbrc.2018.03.169>
- Sun, Z., Schwenzer, A., Rupp, T., Murdamoothoo, D., Vegliante, R., Lefebvre, O., Klein, A., Hussenet, T., & Orend, G. (2018). Tenascin-C promotes tumor cell migration and metastasis through integrin $\alpha 9\beta 1$ -Mediated YAP inhibition. *Cancer Research*, *78*(4), 950–961. <https://doi.org/10.1158/0008-5472.CAN-17-1597>
- Sun, Z., Velázquez-Quesada, I., Murdamoothoo, D., Ahowesso, C., Yilmaz, A., Spenlé, C., Averous, G., Erne, W., Oberndorfer, F., Oszwald, A., Kain, R., Bourdon, C., Mangin, P., Deligne, C., Midwood, K., Abou-Faycal, C., Lefebvre, O., Klein, A., van der Heyden, M., ... Orend, G. (2019). Tenascin-C increases lung metastasis by impacting blood vessel invasions. *Matrix Biology*, *83*, 26–47. <https://doi.org/10.1016/j.matbio.2019.07.001>
- Thomas, D., Rathinavel, A. K., & Radhakrishnan, P. (2021). Altered glycosylation in cancer: A promising target for biomarkers and therapeutics. *Biochim Biophys Acta Rev Cancer*. <https://doi.org/10.1016/j.bbcan.2020.188464>
- Wang, H., Shen, Y., Zhao, L., & Ye, Y. (2020). 1-Deoxynojirimycin and its Derivatives: A Mini Review of the Literature. *Current Medicinal Chemistry*, *28*(3), 628–643. <https://doi.org/10.2174/0929867327666200114112728>
- Wang, R. J., Yang, C. H., & Hu, M. L. (2010). 1-Deoxynojirimycin inhibits metastasis of B16F10 melanoma cells by attenuating the activity and expression of matrix metalloproteinases-2 and -9 and altering cell surface

- glycosylation. *Journal of Agricultural and Food Chemistry*, 58(16), 8988–8993.
<https://doi.org/10.1021/jf101401b>
- Welch, D. R., & Hurst, D. R. (2019). Defining the Hallmarks of Metastasis. *Cancer Research*, 79(12), 3011–3027.
<https://doi.org/10.1158/0008-5472.CAN-19-0458>
- Whitelaw, J. A., Swaminathan, K., Kage, F., & Machesky, L. M. (2020). The WAVE Regulatory Complex Is Required to Balance Protrusion and Adhesion in Migration. *Cells*, 9(7), 1–22. <https://doi.org/10.3390/cells9071635>
- Zhang, C., Guo, X., Xu, Y., Han, X., Cai, J., Wang, X., & Wang, G. (2019). Lung metastases at the initial diagnosis of high-grade osteosarcoma: Prevalence, risk factors and prognostic factors. a large population-based cohort study. *Sao Paulo Medical Journal*, 137(5), 423–429. <https://doi.org/10.1590/1516-3180.2018.0381120619>